A Standardized Method for Analysis of *Medicago truncatula* Phenotypic Development[1][W][OA]

Bruna Bucciarelli, Jim Hanan, Debra Palmquist, and Carroll P. Vance*

United States Department of Agriculture, Agricultural Research Service, Department of Agronomy and Plant Genetics, University of Minnesota, St. Paul, Minnesota 55108 (B.B., C.P.V.); United States Department of Agriculture, Agricultural Research Service, Midwest Area Biometrician, Peoria, Illinois 61604 (D.P.); and Australian Research Council Centre of Excellence for Integrative Legume Research, Australian Research Council Centre for Complex Systems, Advanced Computational Modelling Centre, University of Queensland, Brisbane, Queensland 4072, Australia (J.H.)

Medicago truncatula has become a model system to study legume biology. It is imperative that detailed growth characteristics of the most commonly used cultivar, line A17 cv Jemalong, be documented. Such analysis creates a basis to analyze phenotypic alterations due to genetic lesions or environmental stress and is essential to characterize gene function and its relationship to morphological development. We have documented morphological development of *M. truncatula* to characterize its temporal developmental growth pattern; developed a numerical nomenclature coding system that identifies stages in morphological development; tested the coding system to identify phenotypic differences under phosphorus (P) and nitrogen (N) deprivation; and created visual models using the L-system formalism. The numerical nomenclature coding system, based on a series of defined growth units, represents incremental steps in morphological development. Included is a decimal component dividing growth units into nine substages. A measurement component helps distinguish alterations that may be missed by the coding system. Growth under N and P deprivation produced morphological alterations that were distinguishable using the coding system and its measurement component. N and P deprivation resulted in delayed leaf development and expansion, delayed axillary shoot emergence and elongation, decreased leaf and shoot size, and altered root growth. Timing and frequency of flower emergence in P-deprived plants was affected. This numerical coding system may be used as a standardized method to analyze phenotypic variation in *M. truncatula* due to nutrient stress, genetic lesions, or other factors and should allow valid growth comparisons across geographically distant laboratories.

Medicago truncatula has become a model plant for the study of legume biology (Cook, 1999). With the anticipated sequencing of its genome by 2007, its large expressed sequence tag database, and availability of the Medicago Affymetrix GeneChip, essential resources are available to genetically dissect this organism. However, to fully utilize genomic approaches, the Medicago research community requires standardized methods for growth and phenotypic analysis that can be utilized worldwide. A standardized system, similar to that adopted by the Arabidopsis (*Arabidopsis thaliana*) research community, should allow researchers from geographically distant regions to easily and clearly monitor morphological and developmental changes resulting from mutations, biotic and abiotic stress, and other factors, thereby facilitating the standardization of experimental results across laboratories.

The establishment of a standardized baseline for the temporal developmental growth pattern of *M. truncatula* should provide a uniform approach to compare growth of genetic mutants or ecotypes having a developmentally impaired phenotype. The development of a numerical nomenclature coding system provides a means to define specific growth stages in plant development, thereby making it possible to discern and document specifically where changes occur for phenotypically distinct plants. Additionally, a nomenclature coding system may be used to clearly communicate developmental stages without extensive descriptions. It also provides a basis to standardize tissue collection for analysis. A coding system may also be incorporated into a component of the *M. truncatula* plant ontology database, specifically the plant morphological aspect of the database (Blake, 2004). Its numerical and decimal components are conducive to be queried by computational approaches. Numerical coding systems have been instrumental in the genetic analysis of numerous plant systems such as Arabidopsis (Boyes et al., 2001; Mundermann et al., 2005), *Pisum sativum* (Knott, 1987), and various cereals

(Zadoks et al., 1974; Landes and Porter, 1989). They also have been used in breeding programs associated with important agronomic crops (Lancashire et al., 1991). Nomenclature coding systems have been extensively used for describing growth stages in model animal systems as well (Browder, 1980; Wood, 1988; Bate and Arias, 1993).

We have used nutrient stress to simulate changes in whole plant development to assess the effectiveness of a standardized coding system to reproducibly detect morphological changes in plant growth. We have followed shoot and root development of *M. truncatula* from cotyledon to early pod formation when grown under nitrogen (N)- and phosphorus (P)-deficient conditions. These particular stress conditions were chosen because of their major role in plant growth and their implication in nutrient signaling. P, an important plant macronutrient, is immobile in the soil and is a limiting nutrient in many agricultural systems (for review, see Raghothama, 1999; Vance et al., 2003). N, besides being an important plant macronutrient, plays an integral role in the nodulation process, a key aspect of legume biology. Additionally, these two nutrients have been implicated in nutrient signaling involving long-distance communication between the root and the shoot (Forde and Lorenzo, 2001; Liu et al., 2005). Documenting the morphological development of *M. truncatula* under nutrient-stress conditions should lead to a better understanding of the mechanisms behind plant development associated with these nutrients and, in combination with physiological, biochemical, and genetic data, should lead to a better understanding of the molecular mechanisms controlling nutrient perception, root-shoot communication, and nutrient signaling.

The overall goal of this work was to develop a standardized method to characterize the morphological development of *M. truncatula*, line A17 of cv Jemalong. Specifically, our objectives were: (1) to evaluate the temporal developmental vegetative growth pattern of *M. truncatula* under defined conditions; (2) to develop a standardized nomenclature coding system that identifies specific stages in morphological development; (3) to create a developmental structural model of *M. truncatula* that allows phenological and geometric data, from different experiments, to be visualized for ease of comparison; and (4) to validate the use of the nomenclature coding system to identify phenotypic differences when plants are grown under P- and N-stress conditions. This work was meant to create a framework for the future analysis of phenotypic alterations of *M. truncatula* due to either genetic mutations or environmental conditions.

RESULTS

The Numerical Nomenclature Coding System

M. truncatula produces a procumbent, trailing type of growth habit from the combined elongation of the main and axillary shoots. As shoot apices develop, they produce a series of growth units defined as metamers that consist of an internode, leaf, and axillary bud. The main shoot, the primary axis of vegetative growth, initially produces 4 metamers separated by very short immeasurable internodes. Afterward, the internodes of the successively developing metamers elongate, producing additional trifoliate leaves with measurable internodal distances. A spiral type of phyllotaxy is produced in the elongating portion of the shoot. The axillary bud of each metamer has the potential to grow into an axillary shoot. The initiation and growth of these axillary shoots is coordinated with the elongation of the main shoot.

Based on the coding system developed for the quantitative modeling of Arabidopsis by Mundermann et al. (2005), we propose a numerical nomenclature coding system for *M. truncatula* that follows three principal phases of growth: (1) vegetative growth along the main shoot; (2) vegetative growth along the axillary shoots; and (3) the emergence and development of reproductive organs. These particular growth phases were chosen because they divide growth of *M. truncatula* into easily identifiable components, and they provide distinct stages of growth for data collection. We have modified the Arabidopsis coding system proposed by Mundermann et al. (2005) to account for the unique growth pattern displayed by *M. truncatula*. This system documents plant morphological development by following a series of defined growth units representing incremental steps in the progression of whole plant development. It numbers the developing metameric units sequentially along the main and axillary axes of growth and designates position of flower emergence.

The nomenclature coding system starts with the metamer associated with the unifoliate leaf as metamer 1 (m1). The units developing above this are numbered in ascending order with m2 associated with the first trifoliate, etc. The metamers forming axillary shoots developing off of the main axis are coded first according to their main shoot metamer of origin then numbered sequentially starting at the base with 1 (e.g. the axillary shoot associated with m1 that contains 1 unit of growth is designated as m1-1). Floral location is indicated with an "F" preceding the number of its associated metamer of emergence. Flowers emerging from the axils of the main shoot are designated according to the metamer of origin followed by F0 (e.g. floral emergence from m6 is designated as m6-F0). When considering a flower developing along an axillary shoot, it is coded according to the main shoot metamer of origin followed by the axillary shoot metamer of emergence preceded by "F" (e.g. the flower emerging from the axillary shoot associated with m1 and from the axil of m3 of the m1 axillary shoot is coded as m1-F3). The numerical coding system identifying units of *M. truncatula* growth and their location is illustrated in Figure 1. Additionally, the nomenclature coding system defines leaf and reproductive organ development into nine substages (Table I) depicted by a decimal added as an
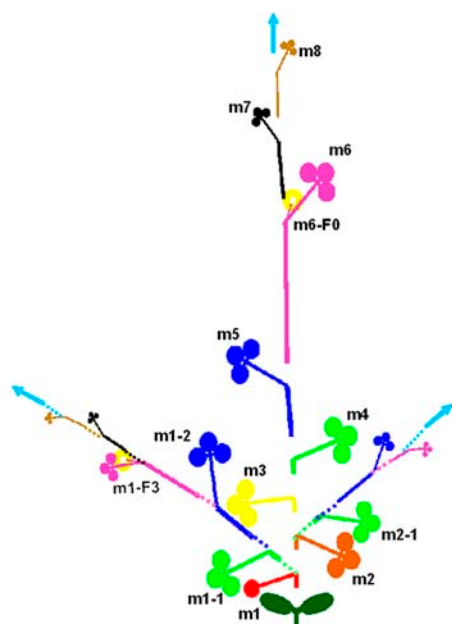
Figure 1. Schematic diagram of *M. truncatula* illustrating the numerical nomenclature coding system. Metamers are labeled along the main shoot and some are labeled along the axillary shoots. The position of flower emergence is designated with an "F" as part of the coding system. Structures sharing a common color (i.e. pink) appear simultaneously. See model animation in Supplemental Figure 2.

extension to the numerical code. These substages were chosen because they are visually identifiable and provide a continuum of growth and development for the organ that they specify. Therefore, to indicate that the m1-1 leaf is fully developed, a code of m1-1.9 is used. A measurement component is also associated with the coding system. Various parameters were measured that could distinguish growth alterations that may be missed by the coding system alone. Plant growth parameters measured for this study included shoot and root fresh and dry weights, shoot and root total lengths, leaf size, and internode lengths. There are numerous other parameters that may have been measured throughout development. The above parameters

were chosen because they are nondestructive and augment the morphological focus of this study.

By following plant growth under nutrient stress conditions, specifically N and P stress, we have simulated potential changes in whole plant development that may occur due to genetic lesions or other factors. This allowed us to demonstrate the use of the coding system and its measurement component to document plant morphological development. Moreover, by using these treatments, we were able to assess the effectiveness of this system to distinguish differences in phenotypic alterations. When shoot tissue of P-deficient and control plants were analyzed for percentage of P, plants grown under P-deficient conditions had a lower P content relative to the controls (compare 0.194% P, SE $\pm$ 0.014, $n = 3$ for P-deficient plants, and 0.462% P, SE $\pm$ 0.042, $n = 3$ for control plants). The low P tissue content in P-deprived plants indicates that the morphological alterations reported in this study can be attributed to the P stress imposed.

The results from this study were also used to construct an empirical model of *M. truncatula* growth and development under these stress conditions. Animations showing model development can be viewed online in Supplemental Figures 1 and 2.

Chronology and Morphological Development of the Main Shoot for *M. truncatula* Grown under Nutrient-Sufficient and -Deficient Conditions

A simple way to orient oneself to the developing plant is to use the unifoliate leaf as a reference marker. The unifoliate leaf, associated with m1, emerges from the developing apical meristem between the two cotyledons (Fig. 2A). The second leaf (associated with m2) emerges 180° opposite to the unifoliate. The developing leaves from m1 and m2, plus the cotyledons, produce a cross type of appearance to the developing plant (Fig. 2, A–C). The third leaf (associated with m3) develops 140° relative to the m2 leaf, adjacent to the m1 leaf. The fourth leaf (associated with m4) develops on the same side of the cotyledons as the m2 leaf and approximately 165° from the m3 leaf (Fig. 2D).

Table I. *Decimal component of the numerical nomenclature coding system of M. truncatula defining leaf and reproductive organ development into nine substages of growth*

Decimal Code[a]	Leaf Developmental Stages[b]	Decimal Code[a]	Reproductive Organ Developmental Stages[b]
0.1	Bud break	0.1	Bud stage
0.2	Blade difficult to discern, visible	0.2	Petals visible, green
0.3	Blade discernible, small	0.3	Petals visible, yellow (closed)
0.4	Blade folded, petiole visible	0.4	Petals open
0.5	Blade half-open	0.5	Petals senescent
0.6	Blade greater than half-open	0.6	Pod visible
0.7	Blade almost fully open	0.7	Pod small (1–5 mm long)
0.8	Blade fully open, green	0.8	Pod medium (>5 mm long), green
0.9	Blade fully open, blue-green	0.9	Pod full size, brown

[a]Decimal numerical code for organ development from emergence to full development.   [b]Definition of decimal code for stages of organ development.

Figure 2. Shoot development of *M. truncatula* grown under nutrient-sufficient (CNT), P-deficient, and N-deficient conditions at 14, 21, and 28 dap. Differences in shoot development at 14 dap are shown for representative plants grown under nutrient-sufficient (A), P-deficient (B), and N-deficient (C) conditions; at 21 dap, nutrient-sufficient (D), P-deficient (E), and N-deficient (F); and at 28 dap, nutrient-sufficient (G) and P-deficient (H). The N-deficient plants at 28 dap have a similar phenotype as that of 21-dap plants; therefore, image is not shown. I, The model rendition of A. J, The model rendition of D. K, The model rendition of plants 40 dap grown under the three nutrient treatments. Leaves associated with metamer growth units are labeled using the numerical nomenclature coding system illustrated in Figure 1. Scale bar = 1 cm. See model animation in Supplemental Figure 1.
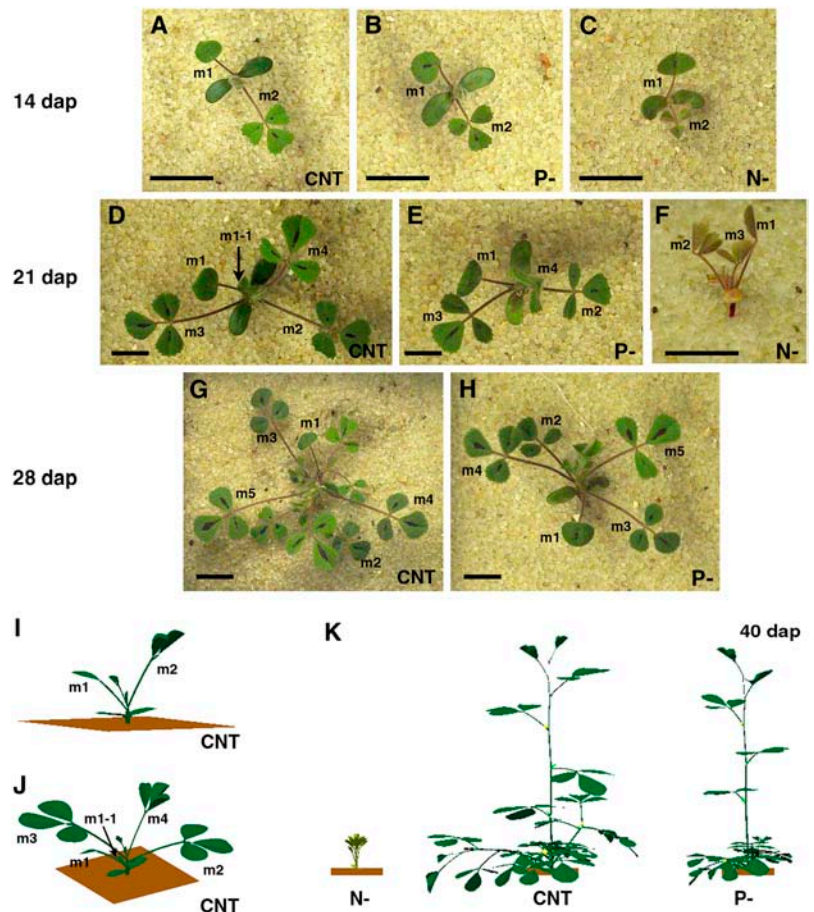

Figure 2 shows metamer location and orientation at key developmental stages of plant growth for the three nutrient treatments (Fig. 2, A–H). Figure 2 also shows the model rendition of some of the key developmental stages plus an empirical reconstruction of plants at 40 d after planting (dap; Fig. 2, I–K). Figure 3 depicts a time line for the chronological progression of plant growth throughout the stages of development over a 40-d period. It includes the time interval to reach key developmental stages and the correlation of these stages with the onset of axillary shoot development and floral emergence. Table II presents a summary of shoot temporal development and the numerical code associated with growth for the three nutrient treatments. It compares growth stage codes and the time it takes to reach these stages. It also shows statistical comparisons of the decimal code for the nutrient-deficient plants relative to plants grown under nutrient-sufficient conditions. An animation of shoot temporal development showing the sequential appearance of shoot structures in a color-coded manner can be viewed online in Supplemental Figure 2.

By 7 dap, there were no visible differences in plant development between the three nutrient treatments (fig. not shown). All plants had fully expanded cotyledons (this occurs by 4 dap) that had a succulent characteristic and were blue-green in color. m1 started to develop as evidenced by the presence of the unifoliate leaf at a mean developmental stage of m1.4, indicating that the unifoliate leaf blade is folded and the petiole is visible (Table I).

By 14 dap, plants grown under both nutrient-sufficient and P-deficient conditions had m1 at full development or near full development (m1.9 and m1.8, respectively) and m2 at a mean developmental stage of m2.7 (Fig. 2, A and B; Table II). However, N-deficient plants began to show a significant delay in development with m1 and m2 (Fig. 2C; Table II; F-test, $P \leq 0.05$). The leaves associated with these metamers stopped developing at a mean leaf developmental stage of m1.5 and m2.5, respectively (half-open position). Furthermore, N-deficient plants were slightly chlorotic, including the cotyledons. Additionally, N-deficient leaf petiole angles, relative to the main axis of growth, were quite acute compared to leaves of the other treatments (compare 36° and 48° from vertical for N deficient and nutrient sufficient, respectively; Fig. 2, A–C). The cotyledons also began to accumulate anthocyanin on their slightly chlorotic surface. Although P-deficient plants showed no significant differences in development relative to nutrient-sufficient plants, some subtle differences were noted.
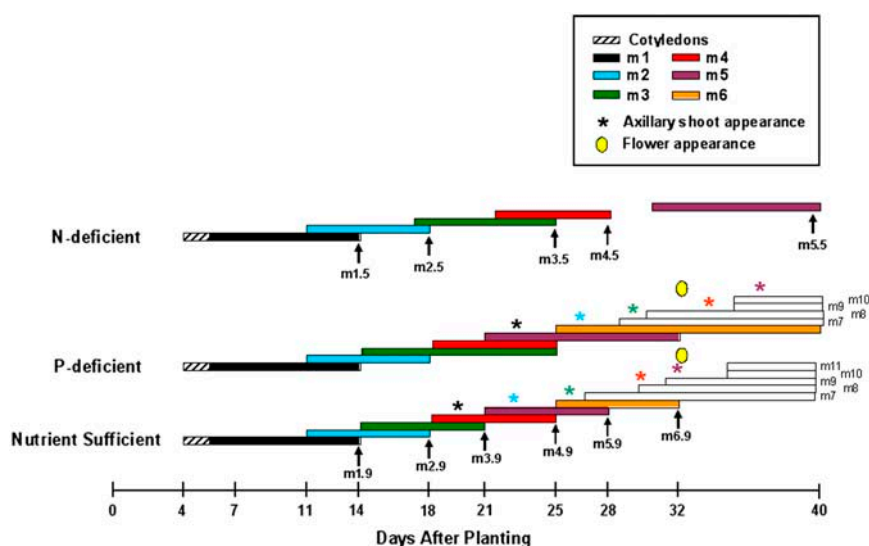
Figure 3. Chronology of metamer appearance along the main shoot of *M. truncatula* over a 40-d period. Plants were grown under nutrient-sufficient, P-deficient, and N-deficient conditions. The first six metamers are color-coded as shown in the legend. Time of axillary shoot appearance is depicted by an asterisk and color-coded according to its metamer of origin. Time of flower appearance is indicated by a yellow oval. The nomenclature code of most metamers, at completion of growth, is labeled and indicated with an arrow.

Specifically, P-deficient plants began to develop patches of anthocyanin on the cotyledon surface, and plants began to appear diminished in size (Fig. 2B).

By 21 dap, the leaf of m3 control plants had a mean developmental stage of m3.9 (Fig. 2D; Table II). Under P-deficient conditions, this leaf was at a mean developmental stage of m3.7 (Fig. 2E; Table II). This is the first sign of a significant developmental difference between nutrient-sufficient and P-deficient plants as detected by the nomenclature coding system (F-test, $P \leq 0.05$). For N-deficient plants, m3 was at a mean developmental stage of m3.4. It should be noted that by 21 dap, the cotyledons of the N-deprived plants showed extreme chlorosis, additional accumulation of anthocyanin, and tissue senescence. The petiole angle of −N plants, relative to the main axis, continued to be acute compared to the other treatments (Fig. 2F). Cotyledons of the P-deprived plants continued to show chlorosis and anthocyanin accumulation on their surface. Cotyledons of control plants showed no change in appearance; they maintained their succulent characteristic and blue-green color. At 21 dap, the mean developmental stage of the leaf associated with m4 showed significant differences in development between plants grown under nutrient-sufficient and P-deficient conditions (Fig. 2, D and E). For control plants, this leaf was at a mean developmental stage of m4.6. Whereas for P-deprived plants mean leaf developmental stage was at m4.4, for N-deficient plants this leaf was just beginning to emerge and was at a mean developmental stage of m4.2.

By 28 dap, the leaf associated with m5 was at a mean developmental stage of m5.9 for plants grown under nutrient-sufficient conditions and at m5.7 for P-deficient plants (Fig. 2, G and H; Table II). It should be noted that by 28 dap, the cotyledons of P-deficient plants were clearly chlorotic and some showed signs of senescence. For N-deficient plants, m5 was not visible until 32 dap (Fig. 3; Table II).

By 32 dap, the leaf associated with m6 for control plants was at a mean developmental stage of m6.9, and for P-deficient plants it was at a developmental stage of m6.7. The main shoot developed subsequent metamers between 32 and 40 dap. By 40 dap, a total of 10 to 11 metamers were produced along the main shoot of both nutrient-sufficient and P-deprived plants. In contrast, the N-deficient plants produced only five metamers (Fig. 3; Supplemental Fig. 1).

Chronology and Morphological Development of the Axillary Shoots for *M. truncatula* Grown under Nutrient-Sufficient and -Deficient Conditions

The first axillary bud to break and initiate growth was associated with m1 (Fig. 3; Table II). The m1 axillary bud break was initiated between 18 and 21 dap in plants grown under nutrient-sufficient conditions (Fig. 3; Fig. 2D) and was correlated with the development of m4 along the main shoot. The m1 axillary bud break of P-deficient plants occurred between 21 and 25 dap and was correlated with the development of m5 along the main shoot (Fig. 3). By 40 dap, the axillary shoot of m1 was a mean developmental stage of m1-6.4 and m1-5.5 for plants grown under nutrient-sufficient and P-deficient conditions, respectively. N-deficient plants failed to develop any axillary shoots. It should be noted that axillary shoot elongation began to occur when the third leaf emerged from its growing point.

The second axillary bud to break and initiate growth was associated with m2 (Fig. 3; Table II). The m2 axillary bud break was initiated between 21 and 25 dap in plants grown under nutrient-sufficient conditions and was correlated with the development of m5 along the main shoot. The m2 axillary bud break of P-deficient plants occurred between 25 and 28 dap and was correlated with the development of m6 along the main shoot (Fig. 3). By 40 dap, the axillary shoot of m2 had a mean developmental stage of m2-6.3 and m2-5.4 for

Table II. *Summary of shoot temporal development of M. truncatula grown under nutrient-sufficient, P-deficient, and N-deficient conditions using the numerical nomenclature coding system to characterize development*

NV, Not visible; NA, not applicable.

Tissue[a]	Days[b]	Description of Developmental Stage for Nutrient-Sufficient Plants	Numerical Code		
			Nutrient Sufficient	P Deficient	N Deficient[c]
Main shoot	14	First leaf at full development	m1.9	m1.8	m1.5[d]
	18	Second leaf at full development	m2.9	m2.9	m2.5[d]
	21	Third leaf at full development	m3.9	m3.7[d]	m3.4[d]
	25	Fourth leaf at full development	m4.9	m4.9	m3.5[d]
	28	Fifth leaf at full development	m5.9	m5.7[e]	m4.5[d]
	32	Sixth leaf at full development	m6.9	m6.7[e]	m5.2[d]
Axillary shoots	21	Axillary of m1 when first leaf blade is discernible but small	m1-1.3	NV[d]	NA
	25	Axillary of m2 when first leaf is almost to fully open	m2-1.7	NV	NA
	28	Axillary of m3 when first leaf is folded and petiole is visible	m3-1.4	NV[d]	NA
	32	Axillary of m4 when first leaf is at the half-open stage	m4-1.5	m4-1.1[d]	NA
	32	Axillary of m5 when first leaf is folded and petiole is visible	m5-1.4	NV[d]	NA
	40	Axillary of m6 when first leaf is greater than half-open	m6-1.6	m6-1.6	NA
	40	Axillary of m7 when first leaf is at the half-open stage	m7-1.5	m7-1.4	NA
Main shoot	40	Floral emergence at m5; small pod stage	m5-F0.7	NVd	NA
	32	Floral emergence at m6; petals visible, yellow and closed position	m6-F0.3	m6-F0.1[d]	NA
	32	Floral emergence at m7; petals visible, green	m7-F0.2	m7-F0.1	NA
	40	Floral emergence at m8; open petal stage	m8-F0.4	m8-F0.3	NA
	40	Floral emergence at m9; petals visible, green	m9-F0.2	m9-F0.1	NA
Axillary shoot	NV	Floral emergence at leaf 1 of m1 axillary; not visible	NV	NV	NA
	NV	Floral emergence at leaf 2 of m1 axillary; not visible	NV	NV	NA
	40	Floral emergence at leaf 3 of m1 axillary; small pod stage	m1-F3.7	m1-F3.5	NA
	40	Floral emergence at leaf 4 of m1 axillary; open petal stage	m1-F4.4	m1-F4.2	NA
	40	Floral emergence at leaf 5 of m1 axillary; bud stage	m1-F5.1	m1-F5.1	NA
	NV	Floral emergence at leaf 1 of m2 axillary; not visible	NV	NV	NA
	32	Floral emergence at leaf 2 of m2 axillary; yellow petal and closed	m2-F2.3	NV[d]	NA
	40	Floral emergence at leaf 3 of m2 axillary; open petal stage	m2-F3.4	m2-F3.4	NA
	40	Floral emergence at leaf 4 of m2 axillary; petals visible, green	m2-F4.2	m2-F4.2	NA
	40	Floral emergence at leaf 5 of m2 axillary; bud stage	m2-F5.1	m2-F5.1	NA
	NV	Floral emergence at leaf 1 of m3 axillary; not visible	NV	NV	NA
	40	Floral emergence at leaf 2 of m3 axillary; visible pod stage	m3-F2.6	m3-F2.2[d]	NA
	40	Floral emergence at leaf 3 of m3 axillary; yellow petal and closed	m3-F3.3	m3-F3.2	NA
	40	Floral emergence at leaf 4 of m3 axillary; bud stage	m3-F4.1	m3-F4.1	NA
	NV	Floral emergence at leaf 1 of m4 axillary; not visible	NV	NV	NA
	40	Floral emergence at leaf 2 of m4 axillary; yellow petal and closed	m4-F2.3	m4-F2.1[d]	NA
	40	Floral emergence at leaf 3 of m4 axillary; bud stage	m4-F3.1	NV	NA
	NV	Floral emergence at leaf 1 of m5 axillary; not visible	NV	NV	NA
	40	Floral emergence at leaf 2 of m5 axillary; bud stage	m5-F2.1	NV	NA

[a]Summary of development is listed by tissue. [b]Days represents days after planting. Plant growth is monitored over 40 d. [c]N-deficient metamers never attain full development. Additionally, axillary shoot and flower emergence do not occur in N-deficient plants. [d]Significant differences at $P < 0.05$. [e]Significant differences at $P < 0.1$.

plants grown under nutrient-sufficient and P-deficient conditions, respectively.

The third axillary bud to break and initiate growth was associated with m3. The m3 axillary bud break was initiated between 25 and 28 dap for plants under nutrient-sufficient conditions and was correlated with the development of m6 along the main shoot (Fig. 3; Table II). The m3 axillary bud break of P-deficient plants occurred between 28 and 32 dap and was correlated with the development of m7 along the main shoot (Fig. 3). By 40 dap, the m3 axillary shoot was at a mean developmental stage of m3-5.4 and m3-4.4 for nutrient-sufficient and P-starved plants, respectively.

Subsequently, the m4 axillary shoot developed between 28 and 32 dap for plants under nutrient-sufficient conditions and between 32 and 40 dap for P-deficient plants (Fig. 3; Table II). Concurrently, m8 and m9 developed along the main shoot. By 40 dap, the m4 axillary shoot was at a developmental stage of m4-4.4 and m4-3.4 for nutrient-sufficient and P-deficient plants, respectively.

Axillary bud break from m5 was initiated by 32 dap in control plants and between 32 and 40 dap in P-deficient plants (Fig. 3; Table II). Axillary bud break from m5 was correlated with the development of m9 and m10 along the main shoot. By 40 dap, the m5 axillary shoot was at the m5-3.4 and m5-2.3 developmental stage for nutrient-sufficient and P-deficient plants, respectively. Axillary buds from m6 and m7 initiated growth just prior to 40 dap for both nutrient

conditions (data not shown). By 40 dap, the m6 and m7 axillary shoots contained 1 leaf.

Flower Emergence along the Main and Axillary Shoots

Flowers began to emerge along the main shoot by 32 dap in both nutrient-sufficient and P-deficient plants (Fig. 3; Table II). However, P-deficient plants had approximately 3-fold fewer flowers that initially emerged at 32 dap, and these flowers were at a significantly younger developmental stage relative to plants grown under nutrient-sufficient conditions (compare mean flower developmental stage of 0.1–0.3, respectively; $n = 11$; t test, $P < 0.05$; Fig. 4A; Table II). Notably, by 40 dap, no differences in number of emerging flowers or their developmental stage was evident for both treatments (Fig. 4A; Table II). The differences in flower number between the nutrient-sufficient and P-deficient plants may be attributed to the delayed development of P-stressed plants because the timing of flower emergence and not position is affected between the two treatments. The initial location of flower emergence for both nutrient-sufficient and P-deficient plants was from the axils of m5, m6, and m7. As the main shoot continued to elongate,

flowers emerged from axils above, but not below, these metamers. N-deprived plants failed to produce any visible reproductive structures.

On elongated axillary shoots, flowers were visible at 32 dap on control plants and at 40 dap on P-deficient plants (Table II). Flowers emerged from elongated axillary shoots that originated from m1, m2, m3, and m4 for both nutrient-sufficient and P-deficient plants. However, plants grown under nutrient-sufficient conditions had nearly 2-fold more flowers that developed from the elongated axillary shoots relative to P-stressed plants (Fig. 4B). Similar to flower emergence along the main shoot, differences in the number of emerged flowers on the elongating axillary shoots may be attributed to the delayed developmental stage of axillary shoots in P-stressed plants relative to the controls. The location of flower emergence along the axillary shoots occurred at a specific metamer from the main shoot metamer of origin and was different for the m1 axillary relative to the other axillary shoots. The first flower to have emerged for the m1 axillary was from the m1-3 position, whereas the first flower to have emerged from the other axillary shoots is from the m2-2, m3-2, and m4-2 positions (Table II). Differences in flower developmental stage between control and P-deficient plants was evident for flowers that emerged from the axillary metamer closest to the main shoot where flowers from the control plants were at a slightly advanced developmental stage relative to the P-deficient plants (Table II). However, such a delay in flower emergence may also be attributed to a delay in axillary shoot development for P-deficient plants. Subsequently, it was difficult to assess whether the delay in flower emergence along the main and axillary shoots for P-deficient plants could be attributed solely to a delay in whole plant development or if a physiological response to P stress could also contribute to such a response.
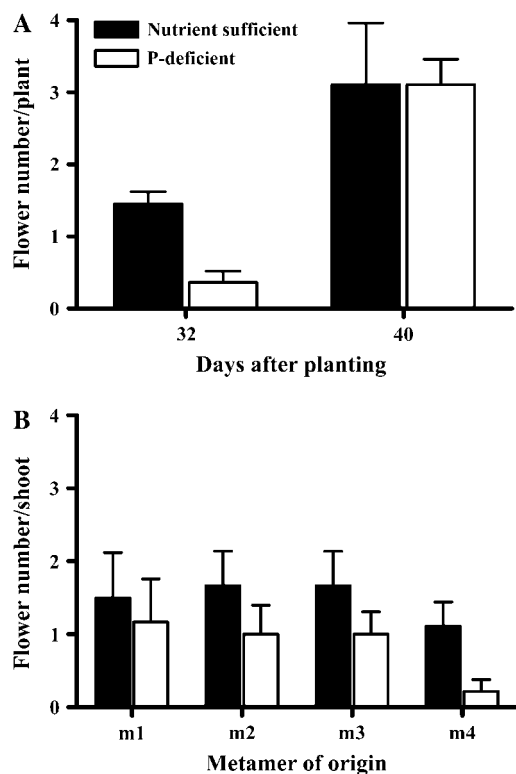
Shoot and Internode Lengths of the Main and Axillary Shoots

Growth parameters for total shoot length, internode length of main and axillary shoots, shoot and root fresh weights, and leaf dimensions were measured every 4 to 7 d beginning at 7 dap. These measurements were used to augment the nomenclature coding system, making the system more sensitive to the identification of phenotypic differences associated with variable treatments.

Main shoot total length and internode lengths were measured at 40 dap for plants grown under nutrient-sufficient and P-deficient conditions. The N-deficient plants failed to produce measurable shoot length and therefore were not included in this analysis. The results showed no significant differences for total length of the main shoot for plants grown under nutrient-sufficient and P-deficient conditions (t test, $P \leq 0.05$). The mean shoot length for plants grown under nutrient-sufficient conditions was 68.7 mm

Figure 4. Flower number along the main and axillary shoots of *M. truncatula* grown under nutrient-sufficient and P-deficient conditions. A, Flower number from main shoot at 32 and 40 dap. Values represent flower number expressed per plant ($n = 11$ for 32 dap; $n = 9$ for 40 dap). B, Flower number from axillary shoots at 40 dap. Axillary shoots are defined by their metamer of origin, m1 to m4, and values represent flower number per axillary shoot ($n = 9$).

(SE ± 13.1, $n = 8$) and for P-deficient condition was 52.6 mm (SE ± 11.6, $n = 9$). Consistent with total shoot length data, no differences were detected for internode lengths of all measurable metamers. Morphologically, a unique pattern of internode elongation emerged along the main shoot regardless of nutrient treatment. Internodes of m1, m2, m3, and m4 were short and immeasurable. However, once the leaf associated with m4 became fully developed, internodes along the main shoot, above m4, began to elongate. Notably, the internode associated with m5 was consistently short (2.2 mm, SE ± 1.11, $n = 9$) relative to other internodes produced above this metamer (e.g. m6 = 15.5 mm, SE ± 3.6, $n = 9$).

Measurement of axillary shoot total length at 40 dap showed that axillary shoots were significantly longer in plants grown under nutrient-sufficient relative to P-deficient conditions (t test, $P \leq 0.05$; Fig. 5A). Axillary shoot internode lengths also appeared to be longer for plants grown under nutrient-sufficient relative to P-deficient conditions (Fig. 5B). However, because of the high variation in internode lengths between plants statistical differences could not be verified.

These results indicate that P deficiency had a greater affect on axillary shoot elongation relative to main shoot elongation. Such a response resulted in P-deficient plants appearing stunted relative to plants grown under nutrient-sufficient conditions. The effect of P deficiency on axillary shoot elongation was not evident until 28 dap and does not affect internodes produced before this time. Therefore, prior to 28 dap, M. truncatula appeared to contain sufficient P to sustain growth comparable to control plants. Whether the lack of difference in main shoot total length would be significant at later stages remains to be established. Perhaps the main shoot was more tolerant of P stress relative to the axillary shoots.

Leaf Dimensions along the Main Shoot

Leaf petiole length, blade length (the length of the middle leaflet including its petiolule), and blade width (distance across the two lateral leaflets including their petiolules) were measured for fully developed leaves associated with m1 through m5 along the main shoot (Fig. 6, A and B).

Leaf petiole lengths were significantly different between the three treatments (F-test, $P \leq 0.05$; Fig. 6A). Differences in petiole length between plants grown under nutrient-sufficient and N-deficient conditions were evident at the m1.9 stage of development. By comparison, differences in petiole length of nutrient-sufficient and P-deficient plants were evident at the m2.9 stage. Petiole length progressively increased as leaves were produced along the main shoot for nutrient-sufficient and P-deficient plants. In contrast, petiole length for N-deficient plants did not vary and remained short relative to the other treatments (Fig. 6A).

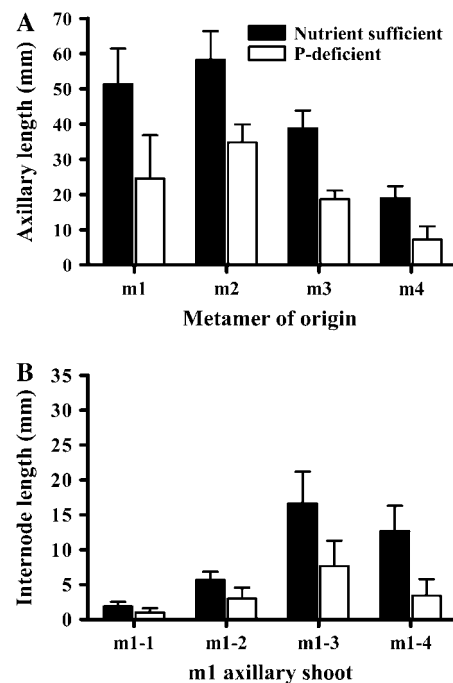Significant differences in blade length were also detected between the three nutrient treatments (F-test,

Figure 5. Axillary shoot total length and internode lengths of *M. truncatula* grown under nutrient-sufficient and P-deficient conditions. A, Axillary shoot total length measured at 40 dap. Axillary shoots are defined by their metamer of origin, m1 to m4. B, Axillary shoot internode lengths for the axillary shoot derived from m1. All internode length measurements taken at 40 dap. Values are means ± SE ($n = 9$). Axillary shoot metamer growth units are defined according to the numerical nomenclature coding system illustrated in Figure 1.

$P \leq 0.05$; Fig. 6B). Plants grown under nutrient-sufficient conditions consistently had longer leaf blades relative to plants grown under P- and N-deficient conditions. Blade length differences between nutrient-sufficient and N-deficient plants were first evident at the m2 position, whereas for P-deficient plants differences were first detected at the m3 position.

Differences in blade width were not detected between nutrient-sufficient and P-deficient plants (data not shown). For N-deficient plants, blade width was difficult to assess because leaf blades failed to completely open.

Root Chronology and Development for *M. truncatula* Grown under Nutrient-Sufficient and -Deficient Conditions

Root architectural development of *M. truncatula* grown under nutrient-sufficient, P-deficient, and N-deficient conditions was analyzed over a 28-d period. Plants were harvested at 4, 7, 14, 21, and 28 dap. Roots were excised and scanned on a flatbed scanner to evaluate root architectural development. Measurements for total length of primary root, first-order laterals, second-, and higher-order laterals were calculated. Additionally, total root number for first-order, second-, and higher-order laterals was also determined. Table
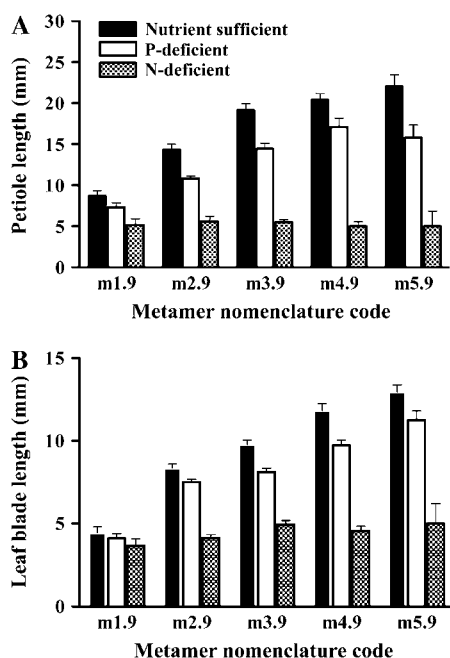
Figure 6. Leaf petiole (A) and blade length (B) comparisons of *M. truncatula* grown under nutrient-sufficient, P-deficient, and N-deficient conditions. All measurements represent leaves at full development from m1 to 5 along the main shoot. Blade length is measured along the midrib of the middle leaflet, including its petiolule. Values represent means ± SE ($n = 9$).

III shows a numerical summary of root growth over a 28-d period as compared to shoot growth stages. Figure 7 illustrates this data in a graphical format. Digital scans comparing *M. truncatula* root architectural development for plants grown under nutrient-sufficient, P-deficient, and N-deficient conditions over a 28-d period can be viewed online in Supplemental Figure 3.

By 7 dap, short first-order lateral roots were visible on all plants regardless of nutrient treatment. There were no differences between the three nutrient treatments when considering primary root length and first-order lateral root total length and total root number (Fig. 7, A–C; Table III).

By 14 dap, second-order lateral roots developed on all plants regardless of nutrient treatment. Second-order lateral root total length and total root number was significantly lower in the N-deficient plants relative to the other nutrient treatments at this time (F-test, $P \leq 0.1$; Fig. 7, D and E; Table III). However, no differences were detectable for primary root length and first-order lateral root total length and total root number, at 14 dap, for all three treatments.

By 21 dap, no differences were detected in first-, second-, and higher-order lateral root total length and number between nutrient-sufficient and P-deficient plants (Fig. 7; Table III). However, for N-deficient plants, first-order lateral root length was significantly shorter and total root number was significantly lower relative to the other two nutrient treatments (F-test, $P \leq 0.05$; Fig. 7, B–E; Table III). Consistent with the previous time point, second- and higher-order laterals for the N-deficient plants continued to be significantly shorter and fewer in number relative to the other treatments.

By 28 dap, differences between nutrient-sufficient and P-deficient plants became visible (Fig. 7, D and E; Table III). Plants grown under P-deficient conditions showed root total length and number lower for second- and higher-order laterals relative to plants grown under nutrient-sufficient conditions (F-test, $P \leq 0.1$).

Table III. *Root growth summary of M. truncatula grown under nutrient-sufficient, P-deficient, and N-deficient conditions*
NA, Not applicable.

Root Type[a]	Days[b]	Shoot Numerical Code[c] Nutrient Sufficient	Root Total Length			Root Total No.[d]		
			Nutrient Sufficient	P Deficient[d]	N Deficient[d]	Nutrient Sufficient	P Deficient[d]	N Deficient[d]
			cm					
Primary root	7	m1.4	4.4 ± 0.4	4.2 ± 0.16	3.9 ± 0.21	NA	NA	NA
	14	m2.7	5.3 ± 0.46	6.7 ± 0.73	6.7 ± 1.64	NA	NA	NA
	21	m3.9	10.4 ± 1.56	9.7 ± 0.87	7.2 ± 0.72	NA	NA	NA
	28	m5.9	NA	NA	10.00 ± 0.94	NA	NA	NA
First-order lateral roots	7	m1.4	3.9 ± 1.14	4.2 ± 0.86	3.6 ± 0.85	4.6 ± 1.05	5.0 ± 0.87	4.1 ± 0.76
	14	m2.7	21.0 ± 1.60	24.5 ± 3.00	25.3 ± 4.24	12.2 ± 0.77	11.5 ± 0.79	12.8 ± 2.25
	21	m3.9	61.0 ± 6.40	64.2 ± 9.02	34.6 ± 5.86[e]	20.4 ± 2.58	20.2 ± 2.54	12.2 ± 1.95[e]
	28	m5.9	118.2 ± 18.52	92.8 ± 15.78	57.0 ± 7.10[e]	15.8 ± 2.39	11.0 ± 2.0	16.5 ± 1.57
Second- and higher-order lateral roots	7	m1.4	NA	NA	NA	NA	NA	NA
	14	m2.7	13.5 ± 2.31	14.0 ± 4.19	2.0 ± 0.63[e]	14.7 ± 1.62	12.0 ± 2.58	2.5 ± 0.84[e]
	21	m3.9	69.4 ± 7.24	72.9 ± 17.55	12.8 ± 2.76[e]	49.7 ± 4.31	50.5 ± 8.98	13.3 ± 1.8[e]
	28	m5.9	244.7 ± 25.76	189.3 ± 17.43[f]	40.5 ± 4.81[e]	133.2 ± 11.79	102.8 ± 11.56[f]	41.2 ± 4.15[e]

[a]Root growth summary is listed by root type.   [b]Days represents days after planting. Root growth summary monitored over 28 d.   [c]The shoot numerical nomenclature code is listed to show shoot developmental stage relative to root growth.   [d]All statistical analyses compared P- and N-deficient treatments to nutrient-sufficient controls.   [e]Significant difference at $P < 0.05$.   [f]Significant difference at $P < 0.1$.

Figure 7. Root growth analysis of *M. truncatula* over 28 d for plants grown under nutrient-sufficient, P-deficient, and N-deficient conditions. A, Primary root total length. B, First-order lateral root total length. C, First-order total lateral root number. D, Cumulative length of second- and higher-order, lateral roots. E, Cumulative number of second- and higher-order, lateral roots. Values represent means ± SE (n = 9).
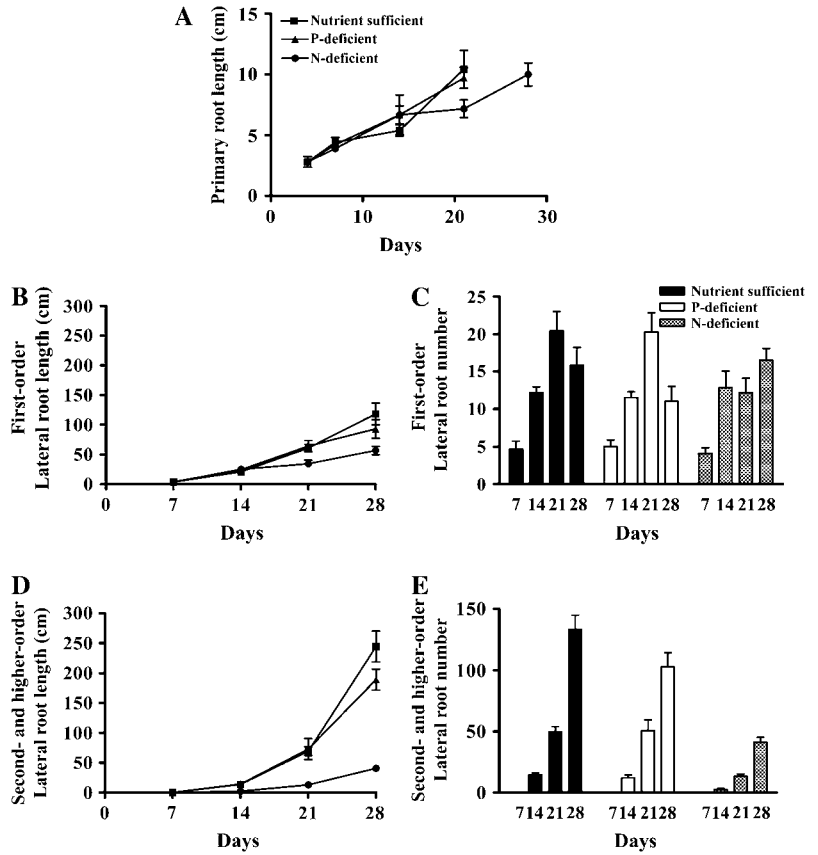
Plants grown under N-deficient conditions continued to have shorter lateral roots relative to the other two treatments. Surprisingly, the number of first-order laterals increased for N-deficient plants but not for the other nutrient treatments. The emergence of first-order lateral roots in N-deficient plants may be related to continued growth of the primary root, whereas primary roots cease developing for the other nutrient treatments.

Shoot-root ratios, based on tissue dry weights, were evaluated at the completion of the study. Shoot-root ratios were similar for plants grown under nutrient-sufficient and P-deficient conditions with a value of 0.9. However, the shoot-root ratio of plants grown under N-deficient conditions was lower with a value of 0.55.

Root hair characteristics were compared between the three nutrient treatments (Fig. 8). Differences in root hair appearance, relative to control plants, were first visible at 14 dap for N-deficient and at 21 dap for P-deficient plants. Root hairs of plants grown under P-deficient conditions (Fig. 8B) were longer relative to their nutrient-sufficient counterparts (Fig. 8A). Additionally, in P-deficient plants, root hair development occurred closer to the root tip in many instances. Root hairs of N-deficient plants were similar in appearance to those of control plants (Fig. 8C). However, the frequency of appearance along the roots varied

between the two treatments. Roots of N-deficient plants had a glabrous appearance, with root hairs either lacking or patchy in distribution.

DISCUSSION

The *M. truncatula* growth analysis and model presented here provide a standardized method to evaluate phenotypic development. In this report, we have: (1) defined a detailed, reproducible baseline description of the temporal growth and developmental pattern of *M. truncatula* from cotyledon to early pod formation; (2) developed a standardized numerical nomenclature
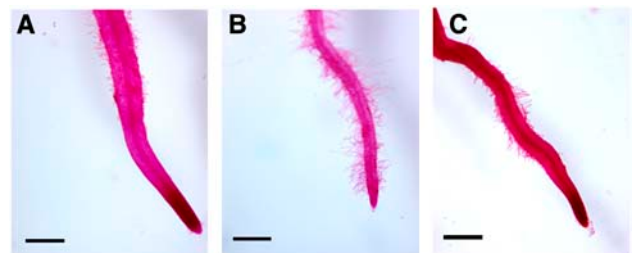
Figure 8. Root hair appearance of *M. truncatula* roots grown under nutrient-sufficient (A), P-deficient (B), and N-deficient (C) conditions. Roots were stained with basic fuschin. Magnification is 20×. Scale bar = 1 mm.

coding system that uses easily identifiable developmental growth stages to define plant growth; (3) identified plant morphological differences resulting from growth under nutrient stress conditions, thereby illustrating how the nomenclature coding system can be used to discern phenotypic alterations; and (4) developed an empirical model of *M. truncatula* development that captures differences in plant structure due to the different nutrient treatments for visualization purposes and provides a framework for future modeling of the genetic and/or physiological mechanisms underlying *M. truncatula* growth and development.

The detailed description of vegetative growth and reproductive organ emergence makes it possible to monitor morphological growth and development because it evaluates plant structures that persist and are visible to the unaided eye. Previous characterizations of *M. truncatula* focused on floral and pod traits (Lesins and Lesins, 1979; Benlloch et al., 2003; Wang and Grusak, 2005). Recently, Moreau et al. (2006) evaluated genotypic variability in *M. truncatula* as a function of thermal time. Their analysis identified changes in *M. truncatula* leaf initiation and appearance on axillary shoots. Our study detailed the chronology and sequential appearance of shoot, root, and flower development over a 40-d period. Such a detailed account of growth provides an architectural model whereby the development of the whole plant can be assessed. It provides an archetype characterization of *M. truncatula* and integrates the growth of the whole plant to the existing knowledge base.

We have created a numerical nomenclature coding system, based on the system outlined by Mundermann et al. (2005) for Arabidopsis, by which changes in morphological and temporal development can be easily monitored. This coding system documents plant morphological development based on a series of defined growth units. We have defined plant growth according to metamer production along the main and axillary axes. These growth units represent incremental steps in the progression of whole plant development. We have documented timing of metamer production over a 40-d period, thereby allowing assessment of alterations in developmental timing. We have included a decimal component to the system that divides metamer growth into nine substages based on leaf or reproductive organ development (Table I). Additionally, a measurement component included in this system helps to distinguish growth alterations that may be overlooked by the coding system alone. The key to detection of subtle changes in growth is to be familiar with whole plant development and its plasticity, compare developmental timing of growth, then monitor and measure growth using various parameters. Regardless of which parameters are monitored, the examination of multiple parameters enhances the potential to detect true phenotypic differences resulting from mutations versus phenotypic plasticity (Coleman et al., 1994; Boyes et al., 2001). This coding system can also be used to standardize tissue collection. Documenting the detailed position from which tissue is harvested and analyzed provides a developmental reference point for comparative analyses across laboratories.

We have validated the effect of the coding system and its measurement component in detecting morphological changes in growth due explicitly to treatment effects over morphological plasticity. Using nutrient stress to modify whole plant development, we simulated changes that may occur due to genetic lesions or other factors. Growth under N and P deprivation produced a number of morphological alterations that could clearly be documented using both the coding system and measurement component. Specifically, N- and P-deprived plants showed a delay in leaf development and expansion along the main and axillary axes of growth (Figs. 2, 3, and 6; Table II), a delay in axillary shoot emergence and elongation (Figs. 2, 3, and 5; Table II), a decrease in leaf and shoot size, and an alteration in root growth (Figs. 5, 6, and 7; Table III). Furthermore, the timing and frequency of flower emergence in P-deprived plants were also affected (Fig. 4; Table II). Both nutrient stress conditions produced similar growth effects; however, the timing, extent, and location of these alterations differed depending upon the nutrient stress imposed.

Most of our results were compatible with and could be integrated into previously published studies that addressed the physiological, biochemical, and genetic mechanisms of plant responses to nutrient stress. When the description of morphological development is integrated with the mechanistic data and viewed in a comprehensive manner, the relationship between function and morphological development can be better realized. For example, the sequential timing of shoot, root, and reproductive structure development of *M. truncatula* grown under P deprivation was similar with reports on P and carbon cycling and remobilization in a variety of plant systems, including *Glycine max*, *Stylosanthes hamata*, *Phaseolus vulgaris*, *Triticum aestivum*, and *Oryza sativa* (Fredeen et al., 1989; Smith et al., 1990; Marschner et al., 1996; Snapp and Lynch, 1996; Peng and Li, 2005; Wissuwa et al., 2005). In our experiments with *M. truncatula* grown under P-deficient conditions, decreased shoot growth and development, detected by 14 dap, were among the first responses observed. The reduction in shoot size was consistent with previously published reports on the effect of P deprivation on plant development. The developing roots become a sink for P and photoassimilated carbon, resulting in these nutrients being partitioned from the shoot to the root, thereby compromising shoot development (Smith et al., 1990; Marschner et al., 1996; Wissuwa et al., 2005). Later in plant development, when flower initiation commences, the flowers/fruit become the major P and carbon sinks, thereby shifting nutrient allocation from the shoot and root into flower/fruit development (Peng and Li, 2005). In our experiments, at 28 dap, just prior to flower emergence at 32 dap, there was a noticeable

decline in root growth. The decreased root growth was consistent with reports that documented flower/fruit development as a new sink, thereby causing the reallocation of nutrients to these developing organs and compromising root growth prior to reproductive structure development (Peng and Li, 2005).

However, not all of our results were consistent with the existing literature. For example, root architectural analysis of *M. truncatula* under P deficiency deviated from that reported for Arabidopsis or *P. vulgaris*, where low P conditions initially increased lateral root length (Lynch and Brown, 2001; Williamson et al., 2001; Al-Ghazi et al., 2003). When we grew *M. truncatula* under P-deficient conditions, there were no detectable differences in root architecture between P-deficient and control plants until 28 dap when P-deficient plants showed a decline in lateral root total length and number relative to control plants. Notably, the increase in lateral root growth reported in other systems was associated with the development of fine feeder-type roots that are also vulnerable to damage upon removal from the growing medium (Hodge, 2004). In our study, some of these fine roots may have been damaged during the process of harvesting. Therefore, a more detailed study of *M. truncatula* root growth using noninvasive techniques and following growth over a shorter period of time would be useful in uncovering subtle spatial and temporal changes in root development due to P stress.

Timing of development in this study has been described in terms of dap, with measurements taken at 4- to 7-d intervals. This means that our models cannot reflect continuous growth of plant parts in detail, as is possible if more frequent measurements are made (Mundermann et al., 2005), but are interpolated linearly based on initiation time, maximum size, and growth duration. For cases where fine details of component growth would be the subject of study, sampling time should be on a shorter time scale, and growth functions fitted to the data should be incorporated in the analysis and model.

An aspect of timing requiring further study is the potential for incorporating the effects of temperature as a driver of physiological processes (Johnson and Thornley, 1985; Hanan, 1997). If *M. truncatula* is grown at different temperatures than those used in this study, the timing of development expressed in days will be different with, for example, lower temperatures, resulting in longer plastochrons. One possibility for dealing with this is to use a technique often used in crop modeling, where temperature and time are integrated into so-called thermal time (Ritchie and NeSmith, 1991; Bonhomme, 2000). This approach assumes that primordia initiation and leaf production responses are linear over a wide range of temperatures. In its simplest form, instead of just counting days, the differences between mean daily temperature and the base temperature below which the plant does not grow are accumulated on a daily basis. Such techniques have been found to be useful in growth analysis

of Arabidopsis leaf development (Granier et al., 2002) and for *M. truncatula* leaf appearance and initiation along axillary shoots (Moreau et al., 2006). The variability of leaf appearance and initiation in *M. truncatula* was minimized when the data were expressed as a function of thermal time versus calendar days (Moreau et al., 2006). Their results show the importance of temperature on development and thereby provide an additional tool by which phenotype may be evaluated.

In conclusion, our results demonstrate the application of a reliable numerical nomenclature coding system plus its measurement component to reveal altered phenotype and development resulting from growth under N and P deficiency. We have demonstrated that our standardized nomenclature coding system describing morphological alterations can be used in conjunction with other results, making it useful for comparative analyses across laboratories and thereby leading to a better understanding of the relationship between plant function and whole plant morphological development. Taken together, the integration of various techniques to study whole plant development can only lead to a more comprehensive understanding of the mechanisms driving the growth of *M. truncatula*.

MATERIALS AND METHODS

Medicago truncatula seeds of line A17 of cv Jemalong were chemically scarified with concentrated sulfuric acid for 8 min and surface sterilized for 3 min with commercial-grade bleach (5.25% sodium hypochlorite). Seeds were given a 2-d germination period at 4°C then transferred to petri plates with moistened filter paper and given a 14-d vernalization period at 4°C. Vernalized seeds with a radical length of 1 to 1.5 cm were planted in pots containing quartz sand. Pot size was 10 cm × 10 cm × 35 cm. Plants were grown at 24°C to 26°C and a 16-h photoperiod (http://www.isv.cnrs-gif.fr/embo01/manuels/pdf/module1.pdf) with a light intensity at the sand surface of 430 to 490 μmol m^{-2} s^{-1}. Plants were fertilized 3 times a week (150 mL of nutrient solution per fertilizer application) with the following nutrient solutions: complete nutrients, final concentration: KNO_3, 15 mM; $Ca(NO_3)_2$ 4H_2O, 12.5 mM; $Ca(H_2PO_4)_2$, 1 mM; $MgSO_4$ 7H_2O, 1 mM; Fe EDTA, 0.01 mM; $MnCl_2$, 0.004 mM; H_3BO_3, 0.02 mM; $ZnSO_4$ 7H_2O, 0.0004 mM; $NaMoO_4$, 0.0001 mM; and $CaSO_4$ 5H_2O, 0.0001 mM. Nutrient solution lacking P substituted Ca ($H_2PO_4)_2$ with 0.74 mM $CaSO_4$ 2H_2O. Nutrient solution lacking N substituted KNO_3 and Ca ($NO_3)_2$ 4H_2O with 12.5 mM K_2SO_4 and 9 mM $CaSO_4$ 2H_2O. Data were collected at 4, 7, 11, 14, 18, 21, 25, 28, 32, and 40 dap. Five seedlings for each treatment were selected for continuous monitoring of shoot growth. These five plants were photographed and various parameters were measured throughout the 40-d period. Plant growth parameters measured included shoot and root fresh and dry weights, shoot and root total lengths, leaf size, and internode lengths. An additional set of plants was grown in parallel for collection and processing of tissue. Total P analysis was done on dried shoot tissue of P-deficient and control plants harvested at 40 dap. Tissue P content was analyzed by optical emission spectroscopy. Three replicated experiments were performed. Images were taken with a Sony DSC-D770 digital camera. Growth angles were calculated from the digital images. All other parameters were measured using a hand-held ruler.

An empirical model of *M. truncatula* development capturing differences in plant structure due to the different nutrient treatments was developed using the L-system-based L-studio software from the University of Calgary (Prusinkiewicz et al., 2000). L-systems are a formalism for describing plant development (Lindenmayer, 1968) that can support a wide range of empirical and mechanistic modeling approaches (Prusinkiewicz, 2004; Mundermann et al., 2005). In L-systems, plant components are represented by an alphabet of symbols with associated parameters. These are arranged in a string that represents the plant structure, with branching topology imposed by a hierarchy of brackets. Growth and development are captured by applying production rules, which describe the changes in components on a daily basis

in this case, to all symbols in the current string to produce a new string representing the plant on the next day. The application of these rules allows development to be visualized in schematic form (Fig. 1) or for the differing architectures to be compared in realistic form (Supplemental Fig. 1). The rules for production of a new metamer (comprised of an internode, a leaf, and an axillary meristem) by an apical meristem are applied after passage of simulated time equivalent to the plastochron or to the branching delay measured for the apex at that position in the plant. Maximum lengths and duration of growth for the individual components are drawn from the empirical data according to the nodal position along the axis, then scaled by the ratio of their age to the duration of growth. More details can be found in the supplemental material technical description and L-system model (Supplemental Fig. 1). This L-system model provides a framework for future modeling of the genetic and/or physiological mechanisms underlying *M. truncatula* growth and development.

To statistically examine developmental scale differences between the treatments, the Levene's test was first performed to satisfy the parametric ANOVA test assumption of homogeneity of variance and normality. A single-factor ANOVA was used to analyze developmental scale treatment differences. If a significant F-test statistic was obtained, then comparisons between each treatment and the control were performed using a Dunnett's test. Additionally, t tests for unequal replication and equal or unequal variances were used for the analysis of leaf and flower developmental scale differences and shoot and internode length differences. For most analyses, differences were considered to be significant at $P \leq 0.05$, but in some instances $P \leq 0.10$ was considered appropriate for distinguishing treatment differences. Data represent the mean of three independent experiments ± SE.

ACKNOWLEDGMENTS

LITERATURE CITED

Al-Ghazi Y, Muller B, Pinloche S, Tranbarger TJ, Nacry P, Rossignol M, Tardieu F, Doumas P (2003) Temporal responses of *Arabidopsis* root architecture to phosphate starvation: evidence for the involvement of auxin signaling. Plant Cell Environ **26:** 1053–1066

Bate M, Arias AM (1993) The Development of *Drosophila melanogaster*. Cold Spring Harbor Laboratory Press, Cold Spring Harbor, NY, pp 4–5

Benlloch R, Navarro C, Beltran JP, Canas LA (2003) Floral development of the model legume *Medicago truncatula*: ontogeny studies as a tool to better characterize homeotic mutations. Sex Plant Reprod **15:** 231–241

Blake J (2004) Bio-ontologies: fast and furious. Nat Biotechnol **22:** 773–774

Bonhomme R (2000) Bases and limits of using 'degree-days' units. Eur J Agron **13:** 1–10

Boyes DC, Zayed AM, Ascenzi R, McCaskill AJ, Hoffman NE, Davis KR, Gorlach J (2001) Growth stage-based phenotypic analysis of Arabidopsis: a model for high throughput functional genomics in plants. Plant Cell **13:** 1499–1510

Browder LW (1980) Developmental Biology. Holt, Rinhart and Winston, Philadelphia, pp 24–31

Coleman JS, McConnaughay KDM, Ackerly DD (1994) Interpreting phenotypic variation in plants. Trends Ecol Evol **9:** 187–191

Cook DR (1999) *Medicago truncatula*: a model in the making! Curr Opin Plant Biol **2:** 301–304

Forde BG, Lorenzo H (2001) The nutritional control of root development. Plant Soil **232:** 51–68

Fredeen AL, Rao IM, Terry N (1989) Influence of phosphorus nutrition on growth and carbon partitioning in *Glycine max*. Plant Physiol **89:** 225–230

Granier C, Massonet C, Turc O, Muller B, Chenu K, Tardieu F (2002)

Individual leaf development in *Arabidopsis thaliana*: a stable thermal-time-based programme. Ann Bot (Lond) **89:** 595–604

Hanan J (1997) Virtual plants: integrating architectural and physiological models. Environ Modelling & Software **12:** 35–42

Hodge A (2004) The plastic plant: root responses to heterogeneous supplies of nutrients. New Phytol **162:** 9–24

Johnson I, Thornley J (1985) Temperature dependence of plant and crop processes. Ann Bot (Lond) **55:** 1–24

Knott CM (1987) A key for stages of development of the pea (*Pisum sativum*). Ann Appl Biol **111:** 233–244

Lancashire PD, Bleiholder H, Van Den Boom T, Langeluddeke P, Stauss R, Weber E, Witzenberger A (1991) A uniform decimal code for growth stages of crops and weeds. Ann Appl Biol **119:** 561–601

Landes A, Porter JR (1989) Comparison of scales used for categorizing the development of wheat, barley, rye and oats. Ann Appl Biol **115:** 343–360

Lesins KA, Lesins I (1979) Genus *Medicago* (Leguminosae). Dr. W. Junk Publishers, The Hague

Lindenmayer A (1968) Mathematical models for cellular interaction in development: parts I and II. J Theor Biol **18:** 280–315

Liu J, Samac DA, Bucciarelli B, Allan DL, Vance CP (2005) Signaling of phosphorus deficiency-induced gene expression in white lupin requires sugar and phloem transport. Plant J **41:** 257–268

Lynch JP, Brown KM (2001) Topsoil foraging: an architectural adaptation of plants to low phosphorus availability. Plant Soil **237:** 225–237

Marschner H, Kirkby EA, Cakmak I (1996) Effect of mineral nutritional status on shoot-root partitioning of photoassimilates and cycling of mineral nutrients. J Exp Bot **47:** 1255–1263

Moreau D, Salon C, Munier-Jolan N (2006) Using a standard framework for the phenotypic analysis of *Medicago truncatula*: an effective method for characterizing the plant material used for functional genomics approaches. Plant Cell Environ **29:** 1087–1098

Mundermann L, Erasmus Y, Lane B, Coen E, Prusinkiewicz P (2005) Quantitative modeling of Arabidopsis development. Plant Physiol **139:** 960–968

Prusinkiewicz P (2004) Modeling plant growth and development. Curr Opin Plant Biol **7:** 79–83

Prusinkiewicz P, Hanan JS, Karwowski MR (2000) L-studio/cpfg: a software system for modeling plants. *In* M Nagl, A Schurr, M Munch, eds, Lecture Notes in Computer Science 1779: Applications of Graph Transformation with Industrial Relevance. Springer-Verlag Press, Berlin, pp 457–464

Peng Z, Li C (2005) Transport and partitioning of phosphorus in wheat as affected by P withdrawal during flag-leaf expansion. Plant Soil **268:** 1–11

Raghothama KG (1999) Phosphate acquisition. Annu Rev Plant Physiol **50:** 665–693

Ritchie JT, NeSmith DS (1991) Temperature and crop development. *In* RJ Hanks, JT Ritchie, eds, Modeling Plant and Soil Systems. Monograph Number 31. American Society of Agronomy, Madison, WI, pp 5–29

Smith FW, Jackson WA, Vanden Berg PJ (1990) Internal phosphorus flows during development of phosphorus stress in *Stylosanthes hamata*. Aust J Plant Physiol **17:** 451–464

Snapp SS, Lynch JP (1996) Phosphorus distribution and remobilization in bean plants as influenced by phosphorus nutrient. Crop Sci **36:** 929–935

Vance CP, Uhde-Stone C, Allan DL (2003) Phosphorus acquisition and use: critical adaptations by plants for securing a nonrenewable resource. New Phytol **157:** 423–447

Wang HL, Grusak MA (2005) Structure and development of *Medicago truncatula* pod wall and seed coat. Ann Bot (Lond) **95:** 737–747

Williamson LC, Ribrioux SP, Fitter AH, Leyer HMO (2001) Phosphate availability regulates root system architecture in Arabidopsis. Plant Physiol **126:** 875–882

Wissuwa M, Gamat G, Ismail AM (2005) Is root growth under phosphorus deficiency affected by source or sink limitations? J Exp Bot **56:** 1943–1950

Wood WB (1988) The Nematode *Caenorhabditis elegans*. Cold Spring Harbor Laboratory Press, Cold Spring Harbor, NY, pp 10–13

Zadoks JC, Chang TT, Konzak CF (1974) A decimal code for the growth stages of cereals. Weed Res **14:** 415–421